Jerome Menegotto, Jean Alié,
Colette Lacabanne and Michel Bauer

Dielectric Study of an Amorphous Pharmaceutical Drug Substance: "Molecular Mobility – Isothermal Crystallization Kinetics" Correlation

introduction

Since last decades, pharmaceutical industries are confronted with the development of the new pharmaceutical drug substances exhibiting in their crystalline forms a particularly slow and/or low solubility in aqueous media. Of all the strategies considered to improve the solubility of new chemical entities (NCE) and so their bioavailability, one of the most promising reckons on the development of drug substances in amorphous form [1-3]. However, due to the high free enthalpy and the significant molecular mobility that characterize disordered phases, low molecular weight systems such as drug substances in amorphous form are well known to be particularly unstable, at least physically, during storage above and below T_g [4,5]. Before trying to stabilize the amorphous phase through different empirical treatments, it seems more appropriate to understand the molecular mechanisms involved in the crystallization process and in a first approach to determine what kind of molecular motions characteristic of the amorphous NCE are responsible for the physical instability.

In this context but also in other domains (polymorphs and solvates characterizations and analyses of complex formulations for example), the contribution of dielectric spectroscopies to study in details all molecular movements specific of amorphous or crystalline phases is essential and probably will become inescapable in the future development of pharmaceutical sciences. In this note, we report briefly recent results obtained on the study of the correlation existing between the molecular mobility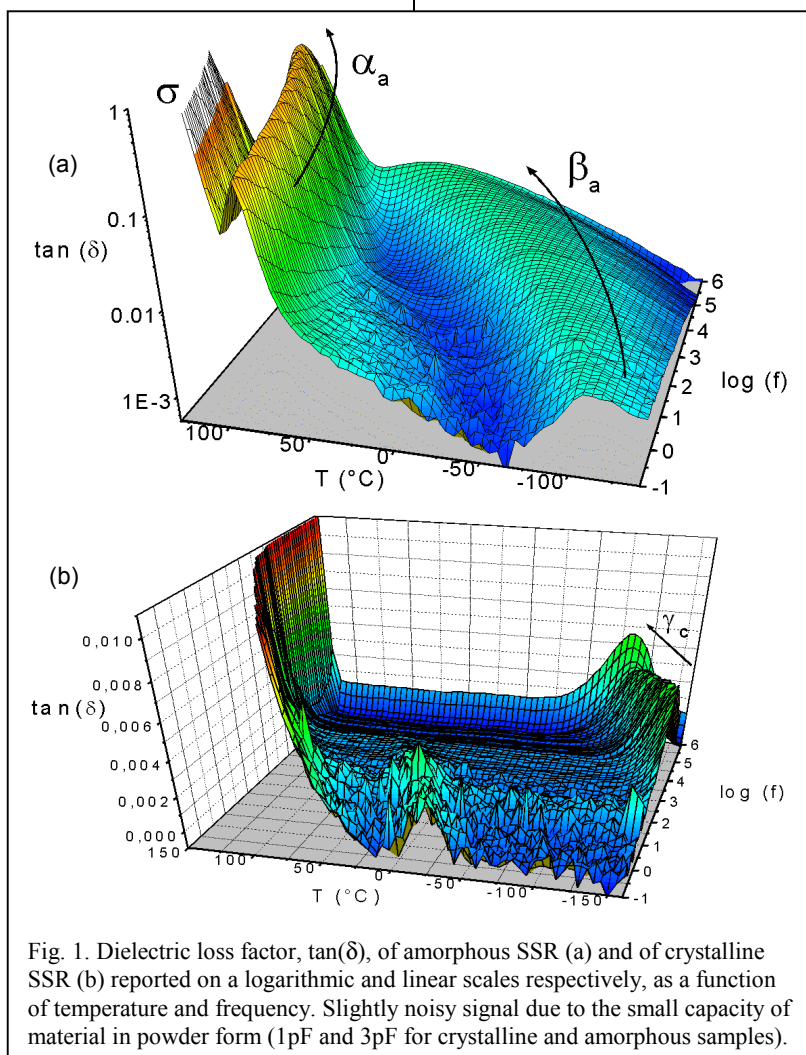 of a model amorphous NCE and its crystallization kinetics determined above and below T_g by dynamic dielectric spectroscopy [6].

model compound

A poorly soluble drug, referred hereafter SSR, in development in Sanofi-Synthelabo Research Department has been selected as a model compound for this study. The amorphous form of SSR was prepared by melting the SSR crystalline form at 180°C for 10 min and then quench cooling the resulting melt in liquid nitrogen. The obtained amorphous film was then ground and stored at 5°C and 0% relative humidity. Further to this thermal treatment, no chemical degradation was detected by high-performance liquid chromatography.

Two different dielectric spectroscopies have been used in this work to study the molecular mobility of compounds in a very broad frequency range: the Dynamic Dielectric Spectroscopy for frequencies between 10^{-1} and 10^6 Hz and the ThermoStimulated Current technique for frequencies between 10^{-3} to 10^{-4} Hz. Complex dielectric permittivity ($\varepsilon^* = \varepsilon'-i\varepsilon''$) and dielectric loss factor ($\tan(\delta) = \varepsilon''/\varepsilon'$) measurements were performed with a Novocontrol Broad Band Dielectric Spectrometer based on a Alpha analyzer and a Quatro temperature controller. The sample was placed into a dielectric cell especially designed for the analysis of powders and low molecular weight systems exhibiting significant flow at high temperatures. The molecular mobility of both crystalline and amorphous forms of SSR were carried out isothermally from –160 to 150°C in steps of 5°C in the $10^{-1} – 10^6$ Hz frequency range. TSC measurements were carried out

Fig. 1. Dielectric loss factor, tan(δ), of amorphous SSR (a) and of crystalline SSR (b) reported on a logarithmic and linear scales respectively, as a function of temperature and frequency. Slightly noisy signal due to the small capacity of material in powder form (1pF and 3pF for crystalline and amorphous samples).

using the fractional polarization method [7-9] in the temperature zone of the thermodynamic glass transition of the SSR drug in amorphous form. Similar sample cells designed to study powder materials were used for TSC experiments.

amorphous and crystalline relaxation

The dielectric properties of amorphous and crystalline forms of SSR are reported in the figures 1.a) and 1.b) respectively. For the amorphous SSR, a weak and broad secondary relaxation mode, noted β_a, was observed in the low temperature range. At high temperature, a more intense and narrow relaxation mode corresponding to the so-called α_a-relaxation associated with the dynamic glass to-liquid transition was observed. As in the case of the amorphous phase, an important dc-conductivity was observed in the high temperature and low frequency range of the dielectric relaxation map of the crystalline SSR. In contrast with the amorphous phase, only one weak relaxation mode, labeled γ_c, was detected in the very low temperature and high frequency range. This relaxation mode corresponds to oscillations of a small dipolar group of the SSR molecules, located in the crystalline phase, not inhibited by strong interactions imposed by neighboring molecules.

To extract the relaxation time of molecular motions involved in both α_a and β_a-relaxation modes by taking into account the conductivity phenomenon and the complexity of each mode, all dielectric spectra were fitted by a sum of Havriliak-Negami (HN) terms with a dc-conductivity contribution: (1)

$$\varepsilon^*(\omega)=\varepsilon_\infty+\sum_j\frac{\Delta\varepsilon_j}{\left[1+\left(i\omega\tau_j\right)^{\alpha_j}\right]^{\beta_j}}+\frac{\sigma_0}{i\varepsilon_0\omega}$$

where ε_∞ is the very high frequency permittivity, σ_0 the dc-conductivity, ε_0 the vacuum permittivity, $\Delta\varepsilon_j$ the dielectric strength, τ_j the relaxation time and α_j and β_j the HN shape parameters of jth relaxation mode ($j = 1$ and 2 for the α_a and β_a relaxations respectively).

The temperature dependence of the HN relaxation times corresponding to the α_a and the β_a-relaxation modes, has been plotted in an Arrhenius diagram shown in the figure 4. Dynamics of elementary relaxation processes resolved by TSC in the T_g temperature domain and involved in the αa-relaxation of the amorphous SSR drug are also

reported on this figure. The temperature dependence of the β_a-relaxation time follows, over the entire frequency-temperature range probed in this work, an Arrhenius law ($\tau = \tau_0\cdot\exp[E/RT]$ with an activation energy $E = 53.2$ kJ·mol-1, pre-exponential factor $\tau_0 = 8.10^{-16}$ s). In contrast, the α_a-relaxation time exhibits a dynamical crossover between a Vogel-Fulcher-Tammann (VFT) law ($\tau = \tau_0\cdot\exp[B/(T-T_0)]$ with $B = 3926$ K^{-1}, $T_0 = -15.7°C$ and $\tau_0 = 2{,}8\cdot10^{-18}$ s) for temperatures $T > T_g$ and an Arrhenius law for $T < T_g$. This Arrhenius-VFT crossover noted for the α_a-relaxation is described by the Adam and Gibbs model [10-12]. The different dynamical behavior determined respectively for the β_a and α_a relaxations are in agreement with the assignment of molecular movements involved in both relaxations. The β_a relaxation has been attributed to localized intra-molecular mobility of SSR molecules (i.e. oscillations of small dipolar groups exhibiting a relative high dipolar moment) and the α_a relaxation has been associated with cooperative movements of molecular clusters and corresponds to the dynamic glass to liquid transition. From the observation of these dynamics, we can conclude that the molecular mobilities of amorphous pharmaceutical drug substances are not really different from the ones currently detected for polymeric materials [13].

The comparison of dielectric responses recorded for the amorphous and crystalline forms of the SSR drug (figures 1.a and 1.b) reveals significant differences between both forms in terms of molecular mobility. These differences are the result of inter and/or intra-molecular interaction strengths that are particularly intensive for the crystal and involve a restricted molecular mobility for organized phases, and weaker for the amorphous phase leading a certain degree of flexibility of molecules in disordered phases. By using a specific molecular mobility of one or the other physical states (amorphous or crystal) as a probe of the quantity of the corresponding state, we can develop amorphous-crystalline or crystalline A – crystalline B forms quantification methods. The exceptional sensitivity of dielectric spectroscopy allows to achieve very low limit of detection (LOD). In the case of amorphous-crystalline quantification, LOD of 1% are currently achieved by Dynamic

Dielectric Spectroscopy (data not shown here).

isothermal crystallization kinetics of the amorphous phase

In this work, the dielectric measurements were also carried out to elucidate the isothermal crystallization kinetics of the SSR drug substance [6]. In this case, we used the ability of the dielectric spectroscopy to detect low amorphous content in a short experimental time (around 1 min) and to follow at a constant temperature as a function of time the quantity of the remaining amorphous phase during crystallization.

It is obvious from the comparison of figures 1.a and 1.b that the frequency-temperature position of the single weak relaxation mode detected for the crystalline form of SSR is outside the range in which the α_a-relaxation mode was detected for the SSR amorphous form. This observation and the high intensity of the α_a-relaxation supports the choice of this relaxation mode to follow the crystallization of the drug substance.

Due to the low frequency shift of the α_a-relaxation process and the long duration of the crystallization process when the temperature is decreased below $T_g = 76°C$, the isothermal cold-crystallization study was performed through two different ways depending of the crystallization temperature, T_c: i) for $T_c > 100°C$, *in situ* real-time isothermal dielectric measurements were carried out at T_c on a unique sample scanned, at successive constant time intervals, in a selected frequency range dependent of T_c and short enough to avoid an evolution of the physical structure of sample during the frequency scan, ii) for $T_c < 100°C$, different amorphous samples were placed on an oven regulated at T_c and at constant time intervals a sample was removed and scanned by Dielectric spectroscopy at 100°C to record dielectric signal of the amorphous phase in a given frequency range in order to quantify the residual disordered phase. As an example, the dielectric properties recorded for SSR initially in amorphous form, at 120°C in the $10^2 – 10^6$ Hz frequency range, for different times between 0 and 41000 s are reported on the figure 2. As expected during the isothermal crystallization of the amorphous phase, for all crystallization temperatures considered in this work (from 50 to 90°C and from 100 to 140°C by steps of 20°C and 5°C
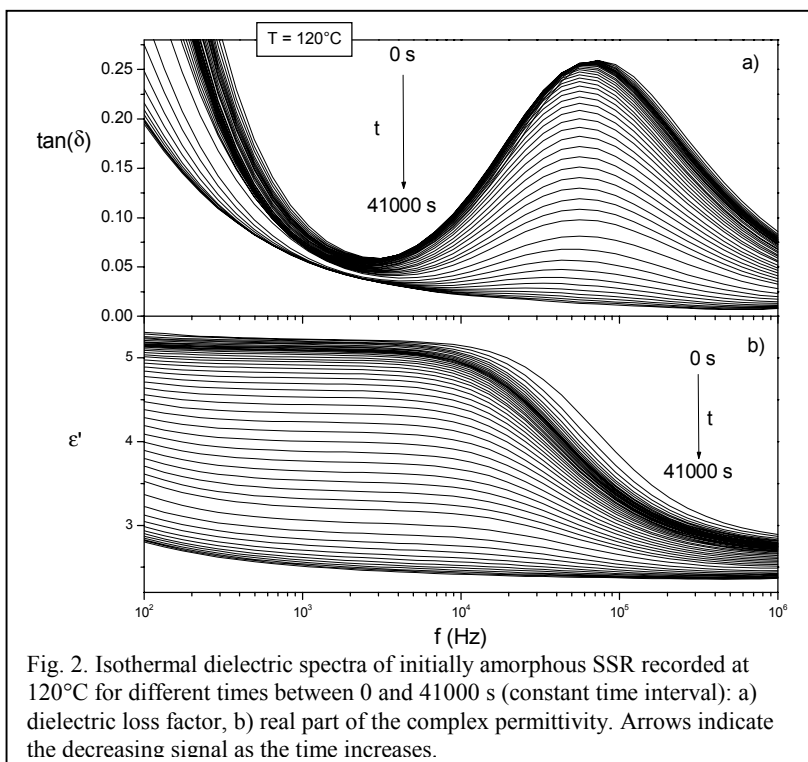
Fig. 2. Isothermal dielectric spectra of initially amorphous SSR recorded at 120°C for different times between 0 and 41000 s (constant time interval): a) dielectric loss factor, b) real part of the complex permittivity. Arrows indicate the decreasing signal as the time increases.

respectively), the decrease of the intensity of the loss peak and the concomitant decrease of the real part increment corresponding to the α_a-relaxation were observed as the experiment time increases after an induction period of time.

phase coupling processes between amorphous and crystalline phases

Whatever the crystallization temperature, the frequency position and the shape of the α_a-relaxation mode are weakly time dependent suggesting that SSR amorphous phase is slightly disturbed by physical constraint imposed by the crystal growth. Depending on the chemical nature of the sample, different results have been reported in the literature regarding this point. For polymers such as poly(ethylene terephthalate) [14] and poly(ether ether ketone) [15] that contain rigid backbones, dielectric spectra shift to low frequency during crystallization, indicating that molecular movements in amorphous phases are significantly restricted by the presence of crystallites. In contrast, for low molecular weight systems [16,17] or polymers with flexible chains, such as poly(L-lactic acid) [18], the molecular mobility of

amorphous phase is unaffected until a high degree of crystallinity is achieved. In the latter case, the confinement effect on the amorphous phase appears as distances between crystallites become shorter than the size of cooperative rearranging regions (CRR) of amorphous phase at the considered crystallization temperature. The difference between the two kinds of materials arises from the propensity of these chemical entities to generate during the crystal growth a strong coupling between both crystalline and amorphous phases for rigid polymers or a soft or null coupling between the two phases for flexible polymers and low molecular weight systems.

In the crystallization study described here, the range of the degree of crystallinity under investigation is low enough to neglect, for this low molecular weight system, the amorphous - crystalline phases coupling and the potential confinement effects. Therefore, it can be considered that this low molecular weight drug crystallizes in a two-phase system. From this reasonable assumption, the degree of crystallinity of the sample was calculated by the determination of the amorphous content from the intensity of the α_a-relaxation mode according to:

$$\chi_c\left(t\right) = 1 - \frac{\Delta\varepsilon\left(t\right)}{\Delta\varepsilon\left(t=0\right)} \quad (2)$$

As expected, the χ_c curves shift to a shorter time as the crystallization temperature increases (figure 3). For each temperature, the characteristic crystallization time was determined from nonlinear least square KWW-Avrami (eq. 3) fits of the $\chi_c(t)$.

$$\chi_c\left(t\right) = 1 - \exp\left[-\left(\frac{t}{\tau_{CR}}\right)^{\beta}\right] \quad (3)$$

correlation of molecular mobility-crystallization kinetics

To find a possible correlation between the molecular mobility of the SSR drug substance in amorphous form and the kinetics of its isothermal crystallization, the characteristic isothermal crystalli-zation time and the relaxation time of both α_a and β_a relaxation modes have been reported on the same Arrhenius diagram (figure 4). The first point to be noted from this figure is the significant difference between the Arrhenius to VFT dynamics of the α_a-relaxation observed below and above T_g respectively and the Arrhenius
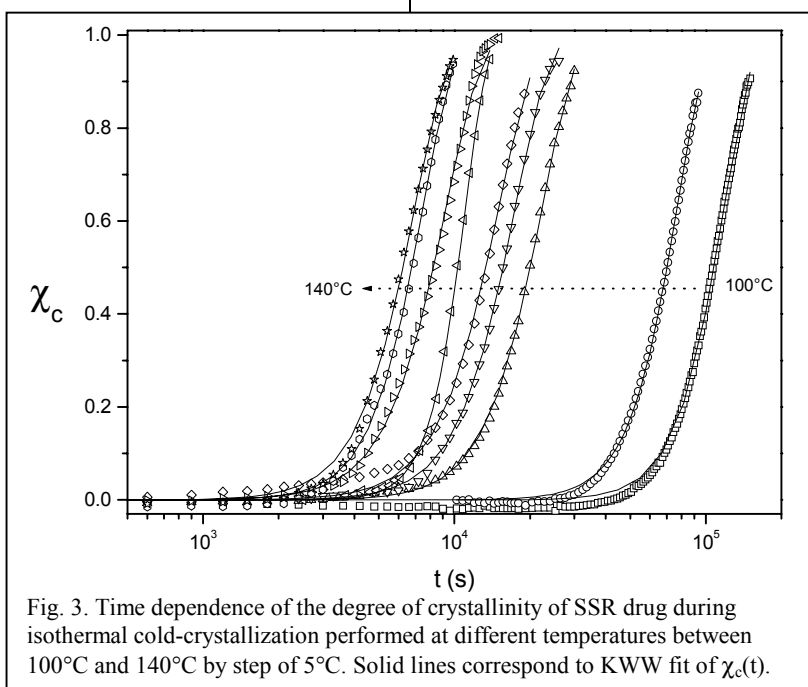

Fig. 3. Time dependence of the degree of crystallinity of SSR drug during isothermal cold-crystallization performed at different temperatures between 100°C and 140°C by step of 5°C. Solid lines correspond to KWW fit of $\chi_c(t)$.

temperature dependence of the τ_{cr} characteristic crystallization time revealed on both sides of T_g. This first point excludes any direct correlation between molecular motions involved in the α_a-relaxation and the isothermal crystallization kinetics. The main point observed in the figure 4 is the connection that can be made between the β_a-relaxation and the crystallization time τ_{cr} that keep the same Arrhenius dynamics over the entire range of investigated temperature above and below T_g. This observation seems to indicate that molecular movements involved in the β_a-relaxation participate in the mechanism of the crystallization of amorphous SSR. This result suggests that, due to their intra-molecular mobility, molecules localized in the amorphous phase near the crystal surface can adjust, during the crystal growth, their local conformation to allow their inclusion in the neighboring crystallite.

To confirm the correlation observed between the intra-molecular mobility of amorphous phases and the crystallization kinetics of these disordered phases and to thereby highlight the mechanism of crystallization, solid state ^{13}C NMR dynamical experiments have been scheduled to characterize in detail the dipolar species involved in the β_a-relaxation of the amorphous SSR drug substance. Another interesting point to confirm the correlation will be the study of the relationship "molecular mobility – crystallization kinetics" for a molecule derived from the SSR drug in which the chemical entity implied in the β_a-relaxation has been replaced.

conclusions

The aim of the study of the molecular mobility – crystallization kinetics correlation is obviously to predict the temperature dependence of the crystallization kinetics of an amorphous drug from the knowledge of the different behavior laws that govern the molecular mobility of the amorphous phase. The influence of specific physical interactions with excipients on the molecular mobility of amorphous drugs and the subsequent influence on the crystallization kinetics will be the next fundamental point to be considered in the future dielectric investigations in pharmaceutical sciences. The results of such studies will help in the preparation of specific pharmaceutical formulations that stabilize drugs in the amorphous
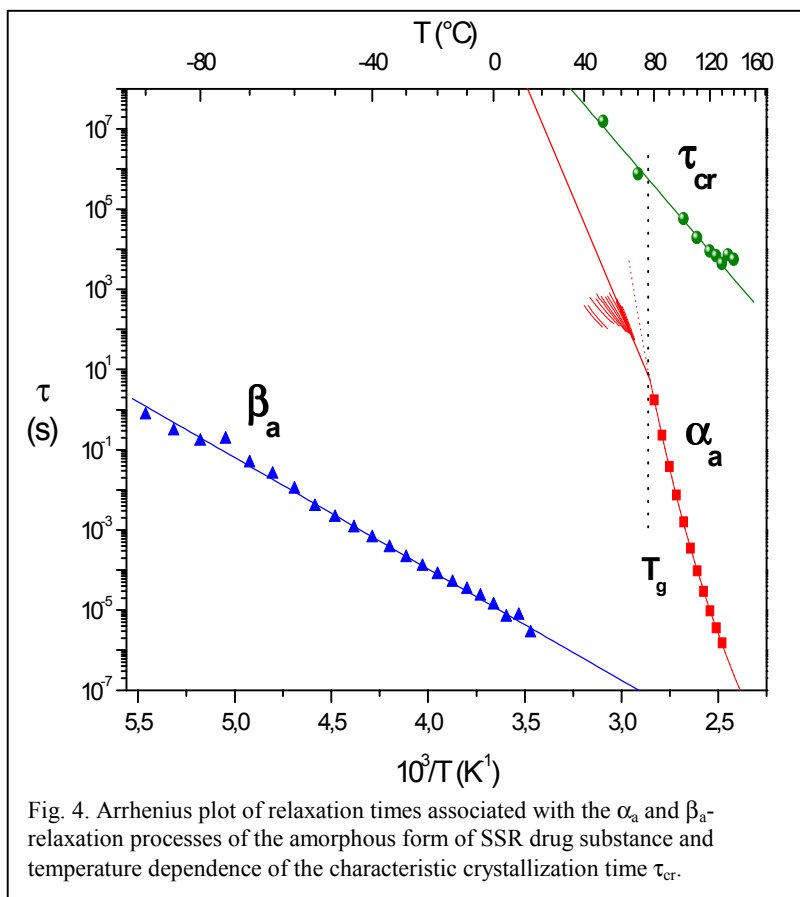

Fig. 4. Arrhenius plot of relaxation times associated with the α_a and β_a-relaxation processes of the amorphous form of SSR drug substance and temperature dependence of the characteristic crystallization time τ_{cr}.

state, which is well suited to clinical purposes.

References

[1] Hancock BC, Zografi G, J. Pharm. Sci. 86:1-12, 1997.

[2] Hancock BC, Parks M, Pharm. Res. 17:397-404, 2000.

[3] Craig DQM, Int. J Pharm. 179:179-207, 1999.

[4] Yu L, Adv. Drug. Delivery Rev, 48:27-42, 2001. Shalaev E, Shalaeva M, Zografi G, J. Pharm. Sci, 91(2):584-593, 2001.

[5] Shalaev E, Shalaeva M, Zografi G, J. Pharm. Sci, 91(2):584-593, 2001.

[6] Alié J, Menegotto J, Cardon P, Duplaa H, Caron A, Lacabanne C, Bauer M, J. Pharm. Sci, 93(1):218-233, 2004.

[7] Menegotto J, Demont P, Bernes A, Lacabanne C, J. Polym. Sci, Part B: Polym. Phys., 37:3494-3505.

[8] Boutonnet-Fagegaltier N, Menegotto J, Lamure A, Duplaa H, Caron A, Lacabanne C, Bauer M, J. Pharm. Sci., 91(6):1548-1560.

[9] Lacabanne C, Lamure A, Teyssedre G, Bernes A, Mourgues M, J. Non-Cryst. Solids, 172-174:884-890, 1994.

[10] Garwe F, Schönhals A, Lockwenz H, Beiner M, Schröter K, Donth E, Macromolecules, 29:247-253, 1996.

[11] Adam G, Gibbs J, J. Chem. Phys, 43(1):139-146, 1965.

[12] Alegria A, Guerrica-Echevarria E, Goitiandia L, Telleria I, Colmenero J, Macromolecules, 28:1516-1527, 1995.

[13] McCrum NG, Read BE, Williams G, Anelastic and Dielectric effects in Polymer solids, Ed. J. Wiley, London, 1967.

[14] Ezquerra TA, Balta-Calleja FJ, Zachmann HG, Polymer 35(12):2600-2606, 1994.

[15] Nogales A, Ezquerra TA, Denchev Z, Sics I, Balta-Calleja, J. Chem. Phys, 155(8):3804-3813, 2001.

[16] Dobbertin J, Hannemann J, Schick C, Pötter M, Dehne , J. Chem. Phys, 108(21):9062-9068, 1998.

[17] Massalska-Arodz M, Williams G, Thomas DK, Jones WJ, Dabrowski R, J. Phys. Chem B, 103:4197-4205, 1999.

[18] Mijovic J, Sy JW, Macro-molecules, 35:6370-6376, 2002.

Jerome Menegotto and Michel Bauer
Sanofi-Synthelabo Research,
Analytical Science Department, 195 Route d'Espagne, 31036 Toulouse Cedex 04, France
Jerome.Menegotto@sanofi-synthelabo.com

Jean Alié and Colette Lacabanne
Polymer Physics Laboratory,
CIRIMAT UMR 5085, P. Sabatier University, 118 route de Narbonne, 31062 Toulouse Cedex, France

Gerhard Schaumburg

Second Generation Alpha-A Dielectric, Conductivity, Impedance and Gain Phase Modular Measuring System

introduction

When Novocontrol introduced the Alpha analyzer in 1998, it was soon accepted by most researchers as the most accurate and versatile analysis tool for dielectric and impedance spectroscopy. The Alpha analyzer combines a series of exceptional features like ultra wide impedance range, frequency range and high accuracy in a fully automated straightforward to handle instrument [1].

These properties result in a new level of performance especially for dielectric spectroscopy applications which are most demanding to measurement equipment. Especially low loss dielectrics and samples with thermally activated isolator conductor transition can be characterized over a broad frequency and temperature range which was not possible before the Alpha analyzer came to the market.

In addition, the typical functionality of a standard impedance analyzer for low impedance samples is supported. The Alpha analyzer is therefore not only the optimal tool for dielectric spectroscopy but due its exceptional overall performance

used by many researches and engineers as an improved analysis tool for other applications, too.

Examples are sensor characterizations where small capacities have to be measured with high precision, analysis of semiconductors, electronic components, bio materials, proteins, organic tissues, cellulose and papers, conductive polymers and organics, ion conductors, fuel cells, power lines, transformer oils and self restoring fuses.

new Alpha-A series combines highest overall performance for both general purpose and special applications

Nevertheless, customers often demanded to combine the Alpha analyzer's exceptional overall performance with additional special functionality like e.g., extended voltage and current range, non linear analysis, high impedance 3- and 4-electrode measurement set-ups, fast measurement rates and DC measurement functionality including potentiostat and galvanostat control functions. From this, the problem arises that due to technical and economical limitations it is difficult to implement this functionality in a single instrument.

With the Alpha-A series which improves the performance of the Alpha analyzer introduced in 1998, Novocontrol now launches a new modular solution which implements all the special applications stated above. The new series is realized as

modular measurement system based on an Alpha-A analyzer mainframe unit which can be connected to a series of test interfaces which are optimized for special functionality. In contrast to many other solutions, all test interfaces are not limited to special functionality but offer highest accuracy, wide impedance and frequency range, too. With this, all interfaces are well suited for a wide range of material measurements from conductors to isolators.

This article gives an overview on the new series and tries to discuss some basic applications. Details of the single interfaces with example measurements will be discussed in following newsletters. A summary including main functions and key specifications can be found in tab. 1 at the end of this article.

extended voltage and current ranges

The two high voltage interfaces HVB 300 and HVB 1000 produce output voltage up to $\pm 150\,V_P$ or $\pm 500\,V_P$ respectively. For high current applications, the two POT/GAL 30V-2A with $\pm 2\,A$ and POT/GAL 15V-10A with $\pm 10\,A$ are available. Within the stated limits any combination of AC and DC voltage or current is supported.

Extended output signals maybe advantageously applied for

• non linear dielectric / impedance spectroscopy;
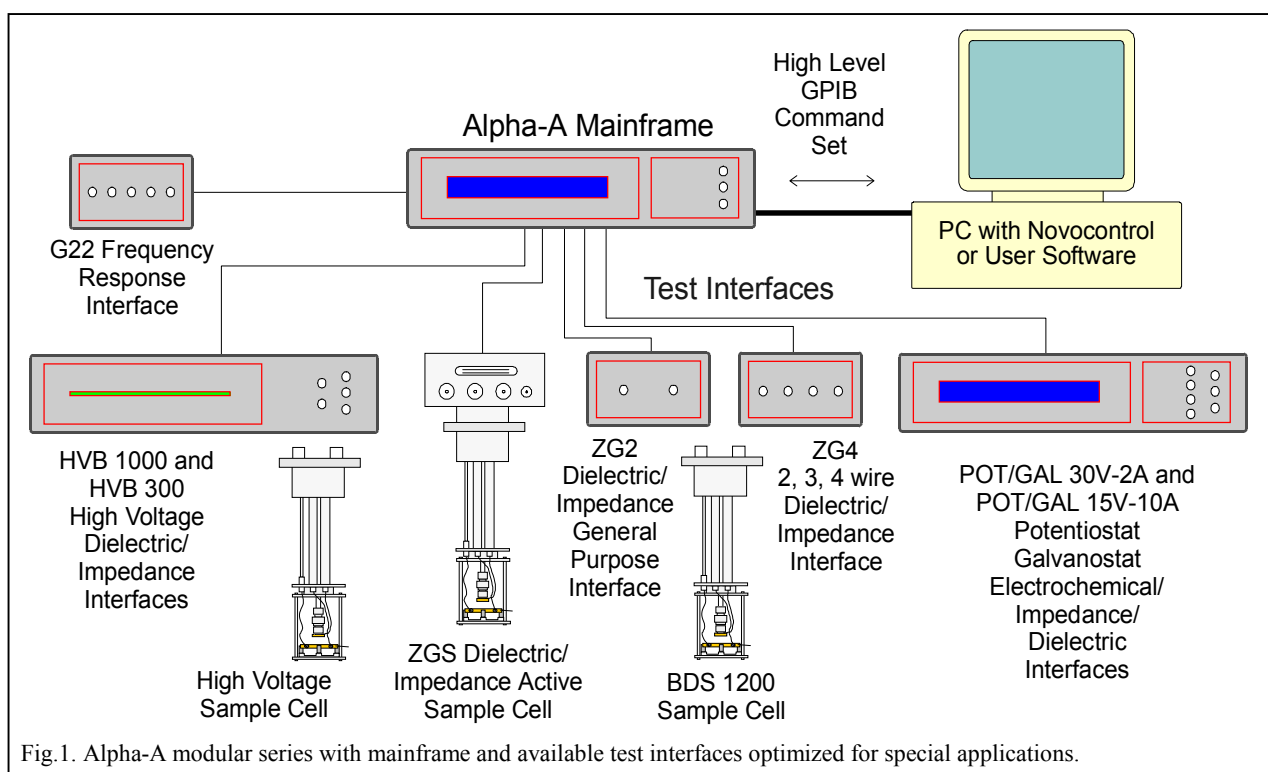• test of materials under stress;
• evaluation of extreme high (high

Fig.1. Alpha-A modular series with mainframe and available test interfaces optimized for special applications.

voltage) or low impedance (high current) materials;

• special technical materials like e.g. fuel cell characterization with the POT/GAL 15V-10A interface.

non linear dielectric and impedance spectroscopy

With the new Alpha-A series, Novocontrol introduces for the first time a turnkey commercial solution for non linear dielectric and impedance spectroscopy. For this purpose, the Alpha-A mainframe and all test interfaces (except G22) support measurements of the sample voltage and current in terms of DC components, harmonic base waves and higher harmonics up to the interface high frequency limit.

Non linear evaluation is fully supported by the Novocontrol WinDETA software, which reads and graphically displays all voltage and current base, and higher harmonic components. In addition, other parameters like DC material parameters, linear impedance, permittivity, conductivity and the corresponding higher harmonic terms are processed.

The higher harmonic current components $I_n^*(\omega)$ are calculated by the Alpha analyzer like the base wave (n=1) by complex Fourier Transform from the sampled current $i(t)$, where n denotes harmonic n-1

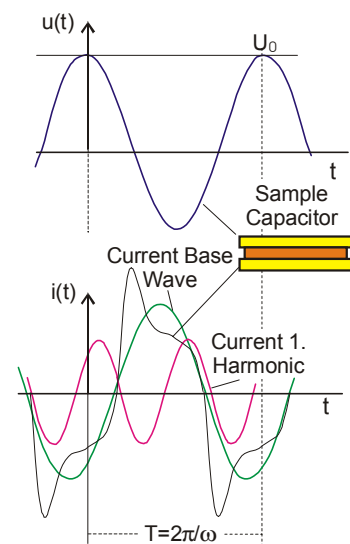$$I_n^*(\omega) = \frac{2}{nT} \int_0^{nT} i(t) \exp(jn\omega t)\, dt \cdot$$

Fig. 2. Sample voltage with non linear response current, current harmonic base wave and first harmonic.

electrode / interface polarization effects

In a measurement of a material prepared between parallel plate electrodes with spacing d, the complex permittivity or conductivity

is evaluated from the phase sensitive measurement of the electrodes voltage difference U_S and current I_S. This method presumes that the applied voltage U_S drops homogeneously within the material by creating a constant electric field $E=U_S/d$.

This presumption does not hold if at the electrode sample interface electrical inhomogeneous layers exist which create a significant voltage drop and by this reduce the E-field in the sample. Such layers may be created by

• accumulation of ions at the electrode for ion conductors like e.g. electrolytes and many liquids (water, electrode polarization);

• bad electrode sample contact connections (contact impedance).

Similar effects may be created by none zero impedance of the cables from the electrodes to the analyzer voltage and current terminals for low impedance samples.

These effects can be in principle cancelled out if separate electrodes for the sample current and voltage measurement are used as shown in fig. 3.
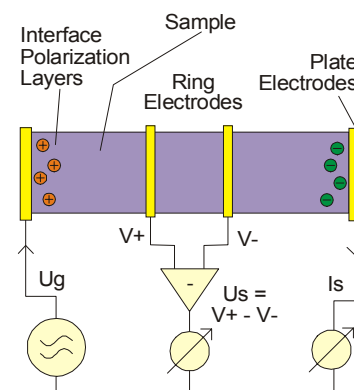

Fig. 3. Principle set-up of a four electrode impedance measurement for electrode - sample interface and cable effects compensation.

The outer two electrodes correspond to the parallel plates of a standard 2-electrode configuration. The voltage is measured by two additional (e.g. ring or needle) electrodes in the inner sample area where no interface effects exist and the field is homogenous.

If the two voltages are measured by an instrument with *infinite input impedance*, no current flows in the voltage electrodes and therefore no ions can accumulate. Due to the zero current, existing contact or cable impedance do not create a voltage drop, too. In this case, the electrical parameters of the material portion between the voltage electrodes can be evaluated without interface polarization and contact or cable

effects from the voltage difference between the voltage electrodes and the current flowing through the outer electrodes. The only, but in practice crucial and not always fulfilled presumption is the sufficient high input impedance of the voltage channels.

The ZG4 and POT/GAL interfaces can in addition to 2-wire- be configured for 3-, or 4-wire measurements. Their input impedance is higher as $10^{12}\,\Omega$ in parallel with 10 pF which exceeds the range of most competing instruments by several orders of magnitude and therefore can be seen as a major improvement in broadband 3- and 4-electrode dielectric/impedance measurements.

On the other hand, especially for high impedance samples at high frequencies the 10 pF input capacity may be in the same order of magnitude as the sample capacity and may contribute to the measured result. 3- and 4-four electrode measurements therefore in practice always require a detailed analysis of the currents flowing into the voltage terminals and the related voltage drop at contacts or electrode interfaces. Details will be discussed in following Dielectrics Newsletters.

electrochemical characterizations

3- and 4-electrode arrangements are often used for electrochemical studies too, where one is not so much interested in the bulk electrolyte but especially in the properties of the polarization layer at the metal to electrolyte or ion conductor interface and the related chemical reactions. This is just the opposite to dielectric / impedance material spectroscopy where these effects are known as electrode polarization which is unwanted and tried to avoid by e.g. 4-electrode arrangements and special cells. The measurement set-up for a typical electrochemical 3-electrode measurement is shown in fig. 4. In addition to the two parallel plate electrodes (denoted as Counter and Working electrode), a third voltage reference electrode is placed close to the polarization layer and measures the voltage difference of the polarization double layer capacity to the working electrode. In contrast to dielectric / impedance material spectroscopy where all electrodes are made of inert metal as e.g. gold, stainless steel or platinum, this applies for the electrochemical cell only for the counter electrode feeding current into the electrolyte.

The working electrode consists of the metal to be characterized in combination with the electrolyte. The reference electrode is usually an open tipped glass capillary filled with a standard electrolyte coupled to a standard metal in order to create a defined electrochemical potential to the electrolyte.
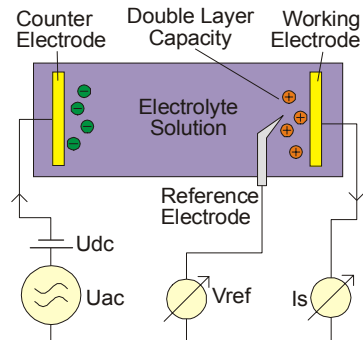

Fig. 4. Principle set-up of a three electrode electrochemical cell for impedance measurement.

The total potential drop across the cell is summed up by all contributions of the chemical process like mass transport, chemical and adsorption steps, electron transfer, etc [2]. By measuring the impedance spectrum $V_{Ref}^{*}(\omega)/I_S^{*}(\omega)$ and fitting it with an equivalent circuit model, the several process contributions can be separated from each other. The typical evaluation includes determination of Warburg impedance related to mass transport, electron transfer resistance, electrolyte resistance and double layer capacity [2].

As on the working electrodes an electrochemical reaction takes place, it is necessary to keep the DC potential V_{Ref} at a defined value or alternatively apply a constant DC current to the cell. This can be done by a Potentiostat / Galvanostat DC circuit as shown in fig. 5. The voltage amplifier connected to CE electrode compares in potentiostat mode the differential voltage $V_{Prc} = V_{RE+} - V_{RE--}$ of both reference electrodes with the intended voltage V_{setDC}. The amplifier adjusts its output voltage until V_{Prc} and V_{setDC} match resulting in a constant and sample impedance independent reference voltage differential which can be adjusted by Vsetdc. In galvanostat mode V_{Prc} is created proportional to the measured cell current by a current to voltage converter (V<-I), resulting in constant sample cell current. In both modes, the variable capacitor C_t adjusts the control loop time constant in order to avoid free high

frequency oscillations caused by too high open loop gain.
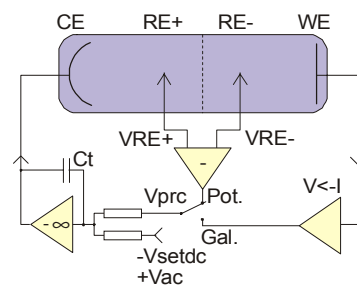

Fig. 5. Principle of Potentiostat / Galvanostat circuit with differential reference voltage inputs.

For impedance measurement an additional small AC voltage V_{AC} is superimposed to V_{setDC} and the AC response is measured as according to fig. 4.

The two new POT/GAL interfaces are optimized for impedance measurements of electrolytes with superimposed controlled voltage or current as described above. The POT/GAL 15V-10A provides up to ±10 A output current and with this is especially suited for fuel cell characterization. POT/GAL 30V-2A is a high quality general purpose instrument. In addition to DC control, the DC voltages and current at the four electrodes are continuously measured and displayed.

In contrast to existing potentiostats /galvanostats for impedance measurement, the POT/GAL interfaces are not restricted to electrolyte characterization but can be used for nearly all other kind of materials, too. E.g. both interfaces support a reference capacitor technique for accurate and broadband measurement of high impedance low loss isolators.

For samples not requiring controlled DC signals, beside the potentiostat and galvanostat a third direct voltage mode is included which bypasses the control amplifier and allows operation like a standard dielectric / impedance analyzer with extended current and voltage range. As a further improvement and new feature, the bandwidth for impedance measurement is not limited by the selected time constant of the DC control amplifier (fig. 5). Instead for any DC bandwidth like e.g. 1 Hz, the full AC impedance frequency range up to 1 MHz is available in both DC controlled modes. Last but not least, both POT/GAL interfaces support fast continuously adjustable simultaneous voltage and current limits of the power amplifier output implemented

independent from the DC control loop, working even in the case of oscillation or reference electrode cable damage in order to protect sensitive samples.

characterization of fast time dependent processes

One major area of dielectric /impedance spectroscopy is monitoring of time variant samples, which is usually due to chemical reactions or crystallization. Examples are time dependent measurements of e.g. epoxy curing or material ageing. Until now, most dielectric analysis systems had data rates in the range of several seconds. This limit is significantly reduced by the new Alpha-A mainframe which is available with a fast data rate option and can measure (and continuously send via the GPIB bus) up to 157 impedance data points per second. This allows process monitoring on time scales below 10 ms. The fast data rates are supported for all test interfaces, but not available for all operation modes like e.g. reference measurement mode or at frequencies < 200 Hz.

For the mainframe standard version (without the fast option) the maximum data rate is up to 10 data points per second.

two electrode standard configurations

For most dielectric or impedance measurements polarization or contact effects as discussed above are less prominent. In this case, the standard configuration with the sample material prepared between two parallel plate electrodes is most advantageous. This arrangement is most simple and allows easy and flexible sample preparation. Nevertheless, the design requirements to an appropriate sample cell operating over a wide frequency, impedance and temperature range without sacrificing the Alpha analyzer's high accuracy are extraordinary demanding.

Such a sample cell in realized as a part of the ZGS interface which is the successor of the popular Alpha-S analyzer active sample cell [1]. In addition to the sample cell, ZGS includes an impedance converter electronics and reference capacitors in the cell head. This arrangement avoids cables in the impedance path between the sample electrodes and analyzer input terminals. Cables may limit the usable high frequency range due to inductance and contribute low frequency noise for high impedance samples.

In contrast to other interfaces and solutions from other manufactures, ZGS is specified at the sample electrodes position and therefore users do not have to care about artefacts by cell contributions to the measured results. The ZGS interface is therefore the optimal and turnkey solution for dielectric and impedance material measurements not requiring three or four electrode configurations.

The ZG2 interface contains the same impedance converter and reference capacitors as ZGS, but no integrated sample cell. ZG2 can be connected by BNC terminals to any passive sample cell like e.g. Novocontrol BDS 1200 or any impedance under test. Compared to ZGS, the combination ZG2 + BDS 1200 is somewhat more flexible but not as accurate due to the additional cables between BDS 1200 and ZG2.

new test interface concept improves flexibility and performance

For the test interfaces a new system concept is realized combining the advantages of a stand alone dielectric / impedance analyzer with the specialized functionality of traditional combined analyzer - interface combinations.

Alpha-A integrated system with automatic interface adaptation and calibration

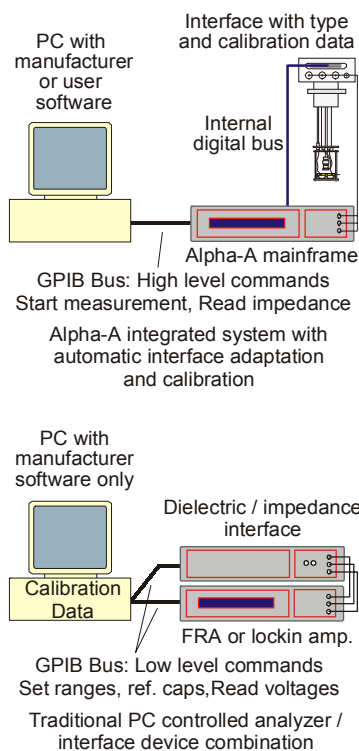Traditional PC controlled analyzer / interface device combination

Fig. 6. System topology for the Alpha-A series and a traditional PC - FRA - interface system

Compared to traditional set-ups the new Alpha-A series has a different system connection topology starting

with one out of a series of interfaces which is connected to the Alpha-A mainframe. The mainframe operates the entire system including low level interface control and high level result evaluation. For this purpose the mainframe is operated by a PC via a set of high level GPIB commands in a flexible and simple fashion.

E. g. a typical command sequence could be: adjust AC voltage and frequency, start measurement, read result as complex impedance or capacity. Depending on the interface type, the mainframe automatically adapts its functionality and command set. E.g. the voltage adjust command will accept voltages up to ±500 V for a HVB 1000 high voltage interface but only ±40V for a ZG2 interface, or special commands for DC polarization control will be available for the POT/GAL interfaces.

The adaptive interface concept allows

• fast low level data exchange and control between the Alpha mainframe and the interface;

• simple and straightforward integration of the Alpha-A system into own written control software or system control packages of other manufacturers.

Though the Alpha-A and all interfaces except G22 are completely integrated in the Novocontrol WinDETA software, operation by other software may be required if the analyzer shall be operated in combination with other equipment (e.g. a synchrotron ring).

This option is an advantage over traditional device combinations for dielectric or electrochemical measurements, where a frequency response analyzer and an interface need to be controlled by a dedicated PC software and the system can not operate without this software as shown in fig. 6.

frequency response, gain phase measurements

In impedance mode used for dielectric / impedance spectroscopy the Alpha analyzer measures the response voltage and current of a material sample to an applied sine wave signal.

In gain phase mode, a second voltage is measured instead of the current. This allows to measure two response voltages to an applied sine wave driver signal at two arbitrary points of a system under test. The two voltages are measured with the Alpha frequency response analyzer

channels CH1 and CH2. The applied sine wave is created by the Alpha sine wave generator.

Gain phase measurements are supported by the Alpha-A mainframe standalone or in combination with any test interface except the two HVB which are for impedance mode only. The G22 interface is for gain phase measurements only and optimized for those applications.

A typical application would be to e. g. measure the transfer function of an amplifier or transformer. In this case, the Alpha generator output and input CH1 have to be connected to the amplifier input and CH2 to the amplifier output. The amplifier complex transfer function defined by V_{out}^{*}/V_{in}^{*} is determined by measuring the voltages at CH2 and CH1.

It should be noted, that in gain phase mode the Alpha can be operated like a digital lock-in amplifier with two input channels. The main function of a lock-in amplifier is to apply a signal with a defined frequency to a system under test and to measure a response signal. As a further lock-in amplifier feature, only the frequency component of the applied generator signal is detected in the response signal. As usually most of the response signals noise and DC errors are at other frequencies, those will therefore be suppressed. The Alpha uses the same principle, but has in addition a second voltage channel, wider bandwidth and better accuracy as lock-in amplifiers.
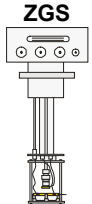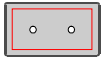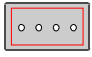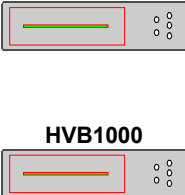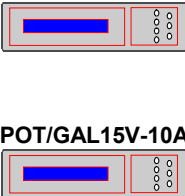
Gain phase measurements are therefore not specially related to dielectric / impedance spectroscopy but may be of general interest if

• a very small or noisy signal has to be measured with high precision;

• the response of any kind of system to an applied signal in the frequency domain has to be measured.

References

[1] G. Schaumburg, Novocontrol, Dielectrics Newsletter, Issue May 1999

[2] Electrochemistry, Carl H. Hamman et. al, Wiley-VCH, 1998, ISBN 3-527-29096-6

Gerhard Schaumburg
Novocontrol Technologies GmbH & Co. KG, Obererbacher Strasse 9, D-56414 Hundsangen, Germany
novo@novocontrol.de

Test Interface	Especially Recommended	Special Features	Key Specification	
ZGS	Dielectric or conductive samples which can be prepared between parallel plate electrodes like e.g. polymers, semiconductors, glasses, and liquids or powders with not to high ion conductivity (electrode polarization). Optimized for broadband measurements of low loss dielectrics over a huge temperature range. Most accurate and straightforward solution for parallel plate electrode configurations.	Included active parallel plate sample cell, specification includes cell effects.	ZGS specs. apply at sample cell electrode position	
			F	$3\ \mu Hz$ - $20\ MHz$
			Z_R	$10\ m\Omega$ - $10^{14}\ \Omega$
			$\tan(\delta)$	$3 \cdot 10^{-5}$; Pa 2 m°
			V_{AC}	$\pm 4{,}2\ V_P$
			V_{DC}	$\pm 40\ V_P$,
				70 mA max
			Z_O	$50\ \Omega$
ZG2	General purpose interface for 2-wire measurements of • dielectric or conductive material samples in combinations with the Novocontrol BDS 1200 parallel plate sample cell; • passive customer own made sample cells; • electronic components.	Fixed 2-wire measurement configuration. Economical version of ZG4 without differential voltage inputs for 3- or 4-wire measurements.	F	$3\ \mu Hz$ - $20\ MHz$
			Z_R	$10\ m\Omega$ - $10^{14}\Omega$
			$\tan(\delta)$	$3 \cdot 10^{-5}$; Pa 2 m°
			V_{AC}	$\pm 4.2\ V_P$
			V_{DC}	$\pm 40\ V_P$,
				70 mA max
			Z_O	$50\ \Omega$
ZG4	Dielectric or conductive samples with • significant electrode contact impedance or electrode sample interface polarization like e.g. electrolytes, liquids with ion conductivity (e.g. water based); • low impedance samples below 1 Ω like e.g. strong electrolytes, heavily doped semiconductors, metals, superconductors; • electronic components or networks.	Selectable 2-, 3- or 4-wire measurement configuration with additional high input impedance and driven shielded V_{high} and V_{low} differential voltage inputs.	F	$3\ \mu Hz$ - $20\ MHz$
			Z_R	$1\ m\Omega$ - $10^{14}\ \Omega$
			$\tan(\delta)$	$3 \cdot 10^{-5}$; Pa 2 m°
			V_{AC}	$\pm 4.2\ V_P$
			V_{DC}	$\pm 40\ V_P$,
				70 mA max
			Z_O	$50\ \Omega$
			Z_{VI}	$10^{12}\ \Omega \parallel 10\ pF$
HVB300 **HVB1000**	Dielectrics, semiconductors or electronic components at high AC and/or DC voltages: • non linear dielectric/impedance spectroscopy • characterization of materials or components under stress; • extreme high impedance samples exceeding $10^{14}\ \Omega$. Optimized for broadband high voltage measurements of low loss dielectrics. Operation with Novocontrol High Voltage Sample Cell recommended.	High AC and/or DC output voltage. Protected against sample breakdowns and permanent shorts.	Z_R	$1\ \Omega$ - $10^{15}\ \Omega$
			$\tan(\delta)$	$3 \cdot 10^{-5}$; Pa 2 m°
			HVB300	
			F	$3\ \mu Hz$ - $1\ MHz$
			$V_{AC}+V_{DC}$	$\pm 150\ V_P$
				70 mA max
			Z_O	$200\ \Omega$
			HVB1000	
			F	$3\ \mu Hz$ - $10\ kHz$
			$V_{AC}+V_{DC}$	$\pm 500\ V_P$,
				3.3 mA max
			Z_O	$150\ k\Omega$
POT/GAL 30V-2A **POT/GAL15V-10A**	• Electrochemical cell reactions, metal electrolyte interfaces, ion conductors , conductive liquids for both low and high impedance samples up to $10^{13}\ \Omega$; • general purpose low impedance samples or electronic components at high currents. Optimized for low impedance samples with strong electrode sample interface polarization effects.	High power superimposed fixed or controlled (Potentiostat) dc voltage or constant DC current (Galvanostat). 2-, 3-, or 4-wire input configuration with driven shields. Simultaneous measurement of DC voltage and current at the four sample terminals. Continuously adjustable output voltage and current limit.	F	$3\ \mu Hz$ - $1\ MHz$
			$\tan(\delta)$	10^{-4}; Pa 6 m°
			Z_R	$1\ m\Omega$ - $10^{13}\ \Omega$
			POT/GAL 30V-2A	
			$V_{AC}+V_{DC}$	$\pm 30\ V_P$, $\pm 2\ A_P$
			Z_O	$1\ \Omega$ - $1\ k\Omega$
			Z_{VI}	$10^{12}\ \Omega \parallel 10\ pF$
			POT/GAL 15V-10A	
			$V_{AC}+V_{DC}$	$\pm 15\ V_P$, $\pm 10\ A_P$
			Z_O	$0{,}1\ \Omega$ - $1\ k\Omega$
			Z_{VI}	$10^{12}\ \Omega \parallel 10\ pF$
G22	High accuracy frequency response and gain phase measurements. Measures the amplitudes and phase shift $V1_{high}$-$V1_{low}$ and $V2_{high}$-$V2_{low}$ of two voltage channels. Similar functionality to a double input channel lockin amplifier with improved accuracy.	Two high sensitive voltage channels with high impedance driven shielded differential inputs. Not for impedance measurements.	F	$3\ \mu Hz$ - $20\ MHz$
			Pa	10 m°
			V_{AC}	$\pm 4.2\ V_P$
			V_{DC}	$\pm 40\ V_P$,
				70 mA max
			Z_O	$50\ \Omega$
			Z_{VI}	$10^{12}\ \Omega \parallel 10\ pF$

Tab. 1. Alpha-A analyzer test interfaces overview. All test interfaces except G22 support automatic reference capacitor measurements and are suited for both dielectric and conductive samples but optimized for special applications. The Alpha mainframe standalone and all interfaces except HVB support two channel high accuracy frequency response or gain phase measurements.

Ranges: F: Frequency, Z_R: Impedance, V_{AC}: AC output voltage, V_{DC}: DC output voltage, $V_{AC}+V_{DC}$: Any combination of |AC output voltage| + |DC output voltage|

Absolute Accuracies $\tan(\delta)$: loss factor, Pa: Phase angle

Other: Z_{VI}: Differential voltage terminals input impedance, Z_O: Power amplifier output impedance

Review of Books on Dielectric Spectroscopy

More detailed information (e.g. table of contents or sample pages) is available on our homepage www.novocontrol.de at the info menu.

Relaxation Phenomena
W. Haase and S. Wróbel

Springer–Verlag, 2003, 716 p. 412 figs, € 245,-

ISBN: 3-540-44269-3

W. Haase, Condensed Matter Research Group, Institute of Physical Chemistry, University of Darmstadt, Darmstadt, Germany.

S. Wróbel, Institute of Physics of the Jagellonian University, Kraków, Poland.

The authors describe the electric, magnetic and other relaxational processes in a wide spectrum of materials: liquid crystals, molecular magnets, polymers, high-Tc superconductors and glasses. The book summarizes the phenomeno-logical fundamentals and the experimental methods used. A detailed description of molecular and collective dynamics in the broad range of liquid crystals is presented. Magnetic systems, high-Tc superconductors, polymers and glasses are an important subject of matter. It is shown that the researchers working on relaxation processes in different fields of materials sciences are dealing with the same physical fundamentals, but are sometimes using slightly different terms.

The book is addressed to scientists, engineers, graduate and undergraduate students, experimentalists and theorists in physics, chemistry, materials sciences and electronic engineering.

Many internationally well known experts contribute to it.

Contents
- Dielectric Relaxation Spectroscopy
- Dynamic Susceptibility of Magnetic Systems
- Relaxation Phenomena in High-Tc Superconductors: Experimental Methods and Results
- Non-chiral Calamitic Liquid Crystals
- Ferro- and Antiferroelectric Liquid Crystals
- Calamitic and Discotic Metallomesogens
- Magnetic Properties and ESR Behavior of Some Molecular Compounds Containing Copper(II) Trimers with the Quartet Spin Ground State
- Magnetic Properties and Relaxations Processes in Manganese(III)-Porphyrins-TCNE-Systems
- Dipolar Interaction and Three-Dimensional Magnetic Ordering of some Chain and Layered Compounds
- Electron Delocalization in Dimeric Mixed-Valence Systems
- High-Tc Superconductors
- Relaxation Phenomena in Nonlinear Optical Polymers
- Relaxation Processes in Two- and Three-Component Metallic Glasses

Electrical Properties of Polymers
E. Riande and R. Diaz-Calleja
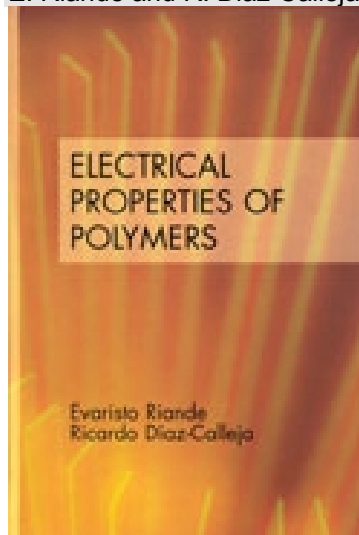
Marcel Dekker, Inc., 2004. Approx. 600 pp. 190 figs. Hardcover, € 195,-

ISBN 0-8247-5346-1

E. Riande, Institute of Science and Technology of Polymers (CSIC), Madrid, Spain.

R. Diaz-Calleja, Department of Applied Thermodynamics ETSII

Polytechnic University of Valencia, Valencia, Spain.

The book presents a systematic and cohesive study of the electrical properties of polymers. The topics covered in this reference/text progress from the physical fundamentals of dielectrics, to structure-property relationships, to molecular dynamics and relaxations.

The properties of liquid crystals, piezoelectric and pyroelectric materials, nonlinear optical polymers, and conducting polymers are discussed in detail.

In-depth and applications-savvy, Electrical Properties of Polymers
- explores the properties of quasi-static dipoles, reviewing Brownian motion, Debye theory, Langevin and Smoluchowski equations, and the Onsager model,
- displays Maxwell, conservation, entropy, and other equations that depict the thermodynamics of dielectric relaxation,
- considers experimental approaches to studying dielectric polymers such as immitance analysis and thermostimulated currents,
- inspects mean-square dipole moments of gases, liquids, polymers, and fixed conformations outlines the principles of electric birrefringence under static fields and clarifies birrefringence dynamics,
- explains molecular dynamics simulations of dynamic dielectric properties, including arrival at the time-dipole correlation coefficient,
- discusses temperature dependence and long- and short-range relaxation dynamics of relaxation processes above glass transition temperature (T_g) or in glassy state.

Contents
- Static Dipoles
- Quasi-Static Dipoles
- Thermodynamics of Dielectric Relaxation in Complex Systems
- Experimental Techniques
- Mean-Square Dipole Moments of Molecular Chains
- Electric Birefringence of Polymers Under Static Fields
- Molecular Dynamics Simulations of Equilibrium and Dynamic Dielectric Properties
- Dielectric Relaxation Processes above Tg
- Relaxations in the Glassy State
- Electric Birefringence Dynamics
- Dielectric Properties of Liquid Crystals
- Piezoelectric and Pyroelectric Materials
- Nonlinear Optical Polymers
- Conducting Polymers

Broadband Dielectric Spectroscopy
F. Kremer and A. Schönhals
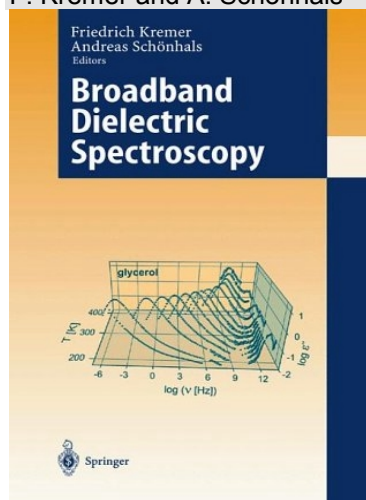
Springer–Verlag, 2003. 729 pp. 393 figs. 22 tabs. Hardcover, € 199,- ISBN 3-540-43407-0

F. Kremer, Institute for Experimental Physics I, University of Leipzig, Germany,

A. Schönhals, Federal Institute of Materials Research and Testing, Unter den Eichen 87, D-12205 Berlin, Germany

It is the intention of this book to be both, an introductory course to broadband dielectric spectroscopy but as well a monograph describing recent dielectric contributions to actual topics, like the scaling of relaxation processes, molecular dynamics in confinement or non-resonant dielectric hole burning, just to name a few. In that the book will correspond to the needs of graduate students but as well to specialized researchers, molecular physicists, polymer and material scientists at university and in industry.

Contents

- Theory of Dielectric Relaxation
- Broadband Dielectric Measurement Techniques (10^{-6} Hz to 10^{12} Hz)
- Analysis of Dielectric Spectra
- The Scaling of the Dynamics of Glasses and Super Cooled Liquids
- Glassy Dynamics Beyond the Relaxation
- Molecular Dynamics in Confining Space
- Molecular Dynamics in Polymer Model Systems
- Effect of Pressure on the Dielectric Spectra of Polymeric Systems
- Dielectric Spectroscopy of Reactive Network-Forming Polymers
- Molecular and Collective Dynamics of (Polymeric) Liquid Crystals
- Molecular Dynamics in Thin Polymer Films
- The Dielectric Properties of Semiconducting Disordered Materials
- Dielectric Properties of Inhomogeneous Media
- Principles and Applications of Pulsed Dielectric Spectroscopy and Nonresonant Dielectric Hole Burning
- Local Dielectric Relaxation by Solvation Dynamics
- Dielectric and Mechanical Spectroscopy - a Comparison
- Dielectric Spectroscopy and Multidimensional NMR - a Comparison
- Polymer Dynamics by Dielectric Spectroscopy and Neutron Scattering - a Comparison

Reviewed by George Fytas

Dielectric spectroscopy has become a mature method almost indispensable in a modern materials lab, where knowledge of the dynamics over a wide frequency range is necessary. After the latest book by McCrum, Read and Williams (1967), an abundance of published work has appeared in a large number of different journals, making increasingly difficult for young researchers a satisfactory and concise introduction to the field. This long-awaited need was made clear in the foreword by the pioneer of the method G. Williams and this book certainly meets that need. F. Kremer and A. Schönhals are experimentalists with leading expertise in the method and its applications in various materials and environments.

This book and the experimental method of the dielectric spectroscopy and its broad spectrum of applications in complex soft matter and glasses monitors overall activities in the last twenty years. In eighteen chapters, the editors have combined in a logical order important experimental contributions from their own research (presented in ten chapters) with the work of other leading scientists employing other complementary spectroscopic techniques as well.

"Broadband Dielectric Spectroscopy" opens with three chapters and the fundamental physical concepts, the experimental techniques used for the measurements of the complex dielectric permittivity over the range 10^{-6} - 10^{12} Hz and the data analysis. These first hundred pages are worth considering as a good text for a graduate course in Materials Science
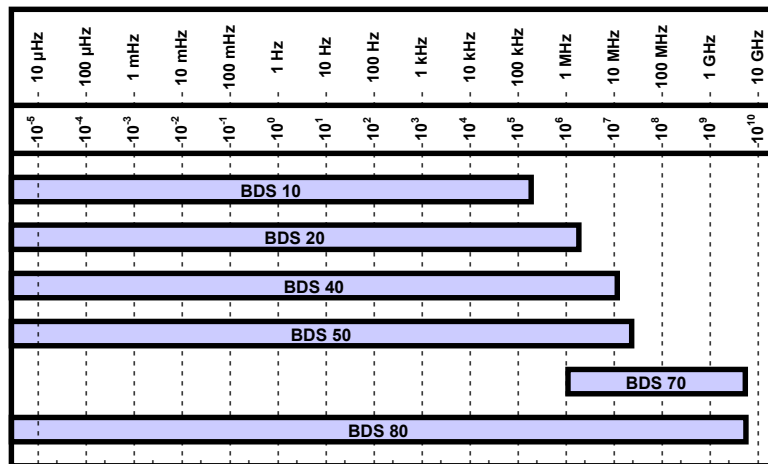
and Engineering Departments. And the knowledge acquired in these chapters is sufficient to navigate through the topics of two related new experimental techniques in chapters 14 and 15.

Contributions of "Broadband Dielectric Spectroscopy" which have been important to condensed matter dynamics are organized around material problems. The vitrification phenomenon of the matter, organic or inorganic, at ambient or under high pressure, is presented in chapters 4, 5, 7 and 8. Four chapters focus on liquid crystals (10), semi conducting materials (12) and multicontituent inhomogeneous systems (9, 13). The open important problem of the dynamic response of molecular and macromolecular materials in confined space and the engrossing topic of thin films prepared by either adsorption or fixed grafting are described in chapters 6 and 11. Due to the paucity of experimental techniques and the lack of consensus, the latter receive a specific weight. The final chapters (16-18) of the book successfully deal with the comparison between Broadband Dielectric Spectroscopy and the established techniques of the dynamic rheometry, NMR and neutron scattering. In this context, only the comparison with photon correlation spectroscopy and optical grating relaxation techniques is missing. And from the materials point of view, the applicability of the dielectric spectroscopy to the study of biological systems is not mentioned either. But given the necessity of selecting, such omissions are justified.

After all developments and numerous applications over the last fifty years dielectric spectroscopy has been established as a powerful experimental method to study collective dynamics in a wide variety of materials. Since 1967, there is a lack of a book which masters the concepts activities and trends of the method in the physics of materials. "Broadband Dielectric Spectroscopy" fills the need diligently. It can serve as valuable centrepiece of an up-to-date advanced graduate course in materials science and help researchers appreciate the potential of the technique which in turn can result in new experimental developments and applications.

OVERVIEW

BROADBAND DIELECTRIC AND IMPEDANCE SPECTROSCOPY
over 16 decades by Novocontrol Technologies

	10 µHz	100 µHz	1 mHz	10 mHz	100 mHz	1 Hz	10 Hz	100 Hz	1 kHz	10 kHz	100 kHz	1 MHz	10 MHz	100 MHz	1 GHz	10 GHz
	10^{-5}	10^{-4}	10^{-3}	10^{-2}	10^{-1}	10^{0}	10^{1}	10^{2}	10^{3}	10^{4}	10^{5}	10^{6}	10^{7}	10^{8}	10^{9}	10^{10}

BDS 10
BDS 20
BDS 40
BDS 50
BDS 70
BDS 80

Factory and Head Office

Germany: NOVOCONTROL TECHNOLOGIES GmbH & Co. KG   Editor Dielectrics Newsletter
Obererbacher Straße 9   Gerhard Schaumburg
D-56414 Hundsangen / GERMANY

Phone: ++49 64 35 - 96 23-0
Fax: ++49 64 35 - 96 23-33   Abstracts and papers are always welcome.
Mail: novo@novocontrol.de   We can publish max. 2 pages A4 on each subject.
Web: www.novocontrol.de   Please send your script to the editor.

Agents

Benelux countries: NOVOCONTROL Benelux B.V. Postbus 231 NL-5500 AE Veldhoven / NETHERLANDS Phone ++(0) 40 - 2894407 Fax ++(0) 40 - 2859209	**Japan:** Morimura Bros. Inc. 2 nd chemical division Morimura Bldg. 3-1, Toranomon 1-chome Minato-Ku, Tokyo 105 / Japan Phone ++(0) 3-3502-6440 Fax: ++(0) 3-3502-6437 Mail hasegawa@morimura.co.jp **Contact:** Mr. Hasegawa
Greece: Theodorou Automation SA 113 Geraka str PO Box 67 868 15344 Gerakas / Greece Tel : ++30 1 6047000 Fax : ++30 1 6046230 email: test@theodorou.gr **Contact:** Mr. George Koukas	**South-East Asia:** ITS Science & Medical Pte. Ltd. 219 Henderson Road #011-02 Singapore 159 556 Phone ++(0) 65 2730-898 Fax ++(0) 65 2730-810 Mail its-sm@its-asia.com **Contact**: Mr. Tony Lee
USA/Canada: NOVOCONTROL America Inc. 611 November Lane / Autumn Woods Willow Springs, North Carolina 27592-7738 / USA Phone: ++(0) 919 639 9323 Toll free: 1-877-639-9323 Fax: ++(0) 919 639 7523 Mail novocontrolusa@earthlink.net **Contact**: Mr. Joachim Vinson, PhD	**Korea:** HI Corporation 3FL, Hoyong Bldg, #1-47 Geumjeong-Dong, Gunpo-City Kyeonggi , Korea 435-824 Phone ++ 82-2-577-1961 Fax: ++ 82 2-577-1963 Mail sunpoint@hanafos.com **Contact**: Mr. Young Hong
Taiwan: JIEHAN Technology Corporation No. 58, Chung Tai East Road, 404 Taichung / Taiwan Phone ++886-4-2208-2450 Fax: ++886-4-2208-0010 Mail jiehantw@ms76.hinet.net **Contact:** Mr. Peter Chen	**People's Rep. Of China:** GermanTech Co. Ltd Room 706, No. 7 Building; Hua Qing Jia Yuan Wu Dao Kou, Haidian District Beijing, 100083 / China Mobile ++ 13501128834 Phone ++(10) 82867920/21/22 Fax: ++(10) 82867919 Mail fwang@germantech.com.cn **Contact:** Mrs. Fang Wang